

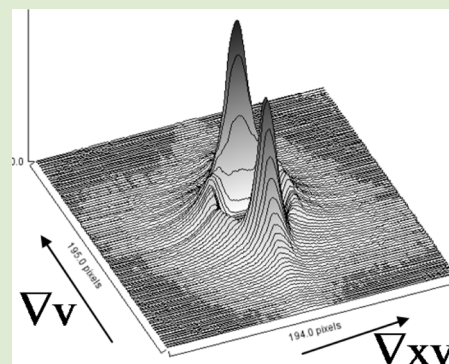
# Large Amplitude Oscillatory Shear Induces Crystal Chain Orientation in Velocity Gradient Direction

K. Sreenivas and Guruswamy Kumaraswamy\*

Complex Fluids and Polymer Engineering, CSIR-National Chemical Laboratory, India

**S** Supporting Information

**ABSTRACT:** Imposition of large amplitude oscillatory shear (LAOS) on crystallizing polymer melts results in lamellar orientation in the shear gradient direction, in contrast to the flow-orientation observed for steady shear. LAOS enhances the formation of plate-like nuclei and orients their normals in the gradient direction. An Arrhenius temperature dependence (with activation energy  $\approx 226$  kJ/mol) characterizes the relaxation of crystal orientation with annealing.



Semicrystalline polymers, such as polyethylene (PE) and isotactic polypropylene (iPP), account for over half of all synthetic polymers produced globally. Melt processing is predominantly employed to convert these polymers into products: the polymer is melted and subjected to forming operations.<sup>1</sup> Subsequently, as the melt solidifies, polymer chains crystallize. Often, the stresses generated in the polymer melt during forming are not fully relaxed as the melt cools and chains crystallize.<sup>1,2</sup> These unrelaxed stresses play an important role in governing polymer crystallization and can accelerate crystallization kinetics by several orders of magnitude relative to quiescent. At the high deformation rates experienced in routine polymer processing operations, oriented crystals form with polymer chains aligned in the flow direction.<sup>2,3</sup> The orientation distribution of polymer crystals significantly influences material properties. For example, highly oriented uniaxially drawn tapes of disentangled ultrahigh molecular weight PE, show a tensile modulus of  $\approx 200$  GPa in the drawing direction, 200 times higher than the modulus of conventional high density PE.<sup>4</sup> Ultradrawn PE nanofibers exhibit thermal conductivities  $\approx 100$  Wm<sup>-1</sup> K<sup>-1</sup> in the fiber direction, 1000-fold higher than “bulk” samples.<sup>5</sup> Therefore, understanding how flow induces crystal orientation is of considerable technological importance.

Semicrystalline microstructure development during various polymer processing operations, such as film blowing, fiber spinning, and injection molding, has been extensively documented.<sup>1</sup> However, the complex thermal and flow conditions that characterize these operations preclude using such experiments to develop a fundamental understanding of flow-induced polymer crystallization. Therefore, researchers have devised model experimental protocols to probe flow-induced crystal nucleation and growth, where isothermal polymer melts are subjected to well-defined flow fields. Several

investigators<sup>6</sup> have employed the “short term shearing” protocol, where stress is applied to an isothermal melt for a brief duration (relative to the crystallization time at that temperature). Short-term shearing experiments probe the effects of stress on early stages of crystallization and, have shown that shear increases the number density of crystal nuclei, consistent with older studies.<sup>7</sup> Above a critical shear stress,<sup>6</sup> highly oriented “shish kebab” crystals develop, with polymer chains oriented in the flow direction forming “shish” that nucleate lamellar “kebab” crystals. The mechanism of shish formation and the factors that govern shish-kebab development, continue to be hotly debated.<sup>6</sup> The exact mechanism of oriented “shish” formation and elaboration in strong flows remains contentious,<sup>6</sup> but there is consensus that when anisotropic polymer crystals form, they align in the flow direction.

Here, we demonstrate that subjecting a polymer melt to large amplitude oscillatory shear (LAOS) results in unusual crystal orientation, with the crystal chain axis oriented along the flow gradient direction. Polymer dynamics theories suggest that, on average, steady shear orients polymer chains along the flow direction.<sup>8</sup> In LAOS experiments, too, orientation of polymer chains in the shear direction has been reported.<sup>9</sup> Therefore, the *gradient* orientation that we observe is highly unusual. In our experiments, a semicrystalline polymer is melted above its equilibrium melting point and, subsequently cooled to a temperature where it is subjected to several cycles LAOS in a 25 mm cone–plate fixture on an ARES strain-controlled rheometer. The shear temperature is selected such that the

**Received:** November 6, 2013

**Accepted:** December 9, 2013

**Published:** December 10, 2013

quiescent crystallization time significantly exceeds the shearing time. Thus, our experiments represent an oscillatory shear analog of the aforementioned short-term steady shear experiments (Supporting Information, Figure S1). After short-term LAOS, the polymer is allowed to crystallize. We report experiments on isotactic polypropylene homo- (iPP) and propylene-ethylene random copolymers (RCP, containing  $\approx 2$  mol % ethylene, detailed characterization in SI, Figures S2–S4).

RCP was melted at 240 °C, then cooled to 132 °C, where it was sheared at a frequency,  $\omega = 1 \text{ rad}\cdot\text{s}^{-1}$  and amplitude,  $\gamma = 500\%$  for 8 cycles of shear (*viz.*, 50.3 s). We carefully examined the sample edge during shearing and note that the sample did not visibly suffer free-surface instabilities or edge failure. The stress response to the imposed oscillatory strain was predominantly at the imposed shearing frequency. The amplitude of the third harmonic of the stress response was over 100-fold weaker, and even harmonics were not observed. Thus, we believe that melt flow instabilities are not responsible for the reported results. After shearing, small amplitude rheology was used to probe the sample as it was isothermally crystallized for 14400 s. At 132 °C, (i) RCP crystallizes in an experimentally tractable time (SI, Figure S5) and (ii) the crystallization time significantly exceeds the shearing time (50.3 s). Imposition of LAOS decreases the time for onset of crystallization ( $t_c$ , characterized by a rapid increase in solid modulus,  $G'$ ) to  $\approx 4300$  s, from the quiescent value  $\approx 11500$  s. Subsequently, the sample was cooled to room temperature and we examined sections cut in the flow-vorticity and gradient-vorticity planes (Figure 1a). Small angle X-ray scattering

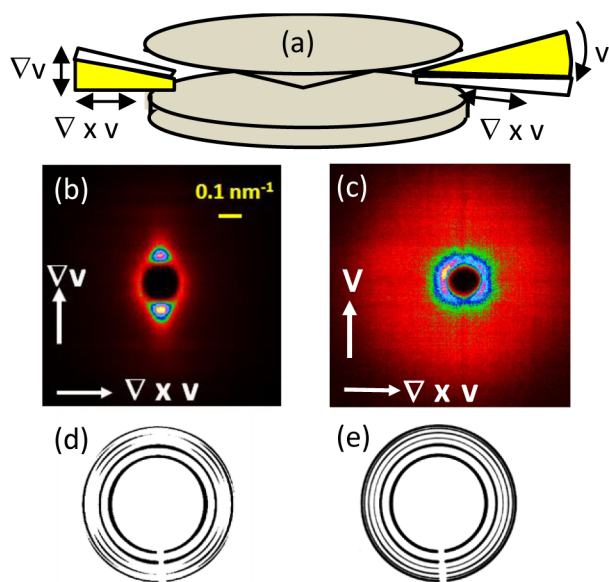


**Figure 1.** (a) Schematic of orientations, obtained by sectioning rheometer samples. X-rays are incident normal to the face shaded yellow. (b, d) SAXS and WAXD, respectively, from the gradient-vorticity plane, while (c) and (e) are the corresponding data in the velocity-vorticity plane.

(SAXS) on samples in the flow-vorticity plane (Figure 1c) showed an isotropic ring at a (Lorentz-corrected) peak position,  $q \approx 0.45 \text{ nm}^{-1}$ , corresponding to crystal lamellae with a long period  $\approx 14$  nm. Remarkably, pronounced anisotropy in the scattering pattern was observed in the gradient-vorticity plane (Figure 1b), with strong lobes along the gradient direction, peaked at  $q \approx 0.4 \text{ nm}^{-1}$ . SAXS in the flow-

shear gradient direction also showed anisotropic scattering, with lobes along the gradient direction (data not presented). Thus, our SAXS data suggests that imposition of LAOS results in uniaxial orientation of crystal lamellae with their axes in the gradient direction. In contrast, imposition of steady shear results in uniaxial orientation in the flow direction, *qualitatively* different from what is observed for LAOS (SI, Figures S6–S8). Wide angle X-ray diffraction (WAXD) indicates unit-cell level anisotropy, that qualitatively mirrors the lamellar-level anisotropy observed in SAXS (Figures 1d,e and S7). Diffraction rings observed in the flow-vorticity plane correspond to  $\alpha$ -phase iPP reflections (110, 040, 130, 111, and  $-131$ ). However, in the flow gradient-vorticity plane, we observe anisotropic crystallization with  $c$ -axis orientation in the gradient direction, mirroring the gradient direction lamellar orientation observed in SAXS.

We have systematically investigated the influence of LAOS conditions on crystal orientation. When RCP was subjected to LAOS ( $\gamma = 500\%$ ;  $\omega = 1 \text{ rad}\cdot\text{s}^{-1}$ ) for increasing cycles of shear,  $t_c$  decreases from  $\approx 11500$  s for quiescent crystallization to  $\approx 9000$ , 6300, and 4300 s for 1, 2, and 8 cycles of shear, respectively (SI, Figure S5). We have calculated the orientational order parameter,  $f = \langle 1/2(3 \cos^2 \phi - 1) \rangle$  from the azimuthal angle ( $\phi$ ) dependence of the  $q = 0.4 \text{ nm}^{-1}$  SAXS peak. Corresponding to the decrease in  $t_c$ ,  $f$  increases from 0 for quiescent crystallization to 0.003, 0.08, and 0.14 for 1, 2, and 8 cycles of shear, respectively (SI, Figure S9). Increase in  $\gamma$  from 125%, 250% to 500% (8 shear cycles,  $\omega = 1 \text{ rad}\cdot\text{s}^{-1}$ ) results in a systematic decrease in  $t_c$ , and increase in  $f$  (SI, Figure S10). The trends in  $f$  and  $t_c$  with  $\gamma$  and cycles of shearing are as anticipated. The influence of frequency is more interesting. We observe that a decrease in LAOS  $\omega$  from  $10 \text{ rad}\cdot\text{s}^{-1}$  to  $1 \text{ rad}\cdot\text{s}^{-1}$  to  $0.1 \text{ rad}\cdot\text{s}^{-1}$  ( $\gamma = 125\%$ , 8 shear cycles) results in an *increase* in  $f$  (from  $\approx 0.05$  to 0.06 to 0.09, respectively) and a decrease in  $t_c$  from  $\approx 9200$  s (*viz.*, only slightly lower than the quiescent  $t_c$ ) to 8400 and 4000 s, respectively (Figure 2 and SI, Figure S11).

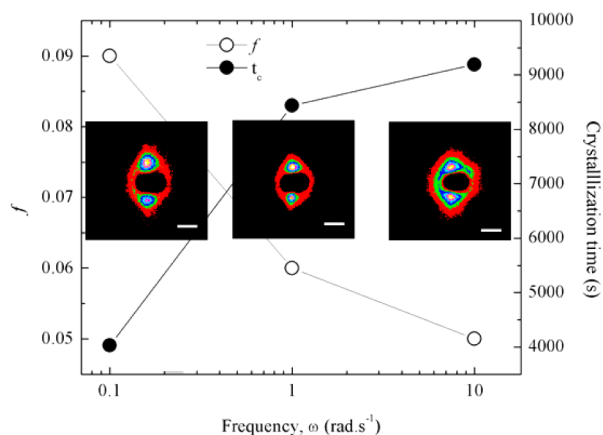


**Figure 2.** LAOS  $\omega$  dependence of crystallization time and  $f$ . Scale bar in the inset (SAXS) corresponds to  $0.1 \text{ nm}^{-1}$ .

Since we seek to keep the shearing times  $\ll t_c$  in our short-term LAOS experiments, imposing a lower  $\omega$  is not practical. We reiterate that the influence of LAOS is *qualitatively* different from steady shear. In short-term *steady* shear experiments, increasing the shear rate results<sup>6</sup> in a dramatic nonlinear decrease in crystallization time and an increase in crystal orientation. For LAOS, not only does the crystal  $c$ -axis orient in the gradient direction, but  $f$  increases as  $\omega$  decreases. Thus,

equivalence between LAOS and steady shear (like the Cox–Merz rule<sup>10</sup>) is inappropriate.

How can we rationalize the unusual gradient orientation and  $\omega$  dependence in short-term LAOS? In short-term *steady shear* experiments,<sup>6</sup> active “point” nuclei form due to the flow-induced orientation of the chain segments. Long chain molecules in the melt, either adsorbed or associated with these point nuclei are stretched in strong flow fields. These initiate the growth of linear “shish” nuclei aligned in the flow direction, that nucleate lamellar “kebab” structures.<sup>6</sup> Thus, the imposed deformation directly couples to polymer chain conformation, explaining the strong nonlinear effect of shear rate. This mechanism cannot explain the LAOS results: (a) in LAOS, chains have been reported<sup>9</sup> to orient in the flow direction, while crystals orient with their chain axis in the gradient direction, and (b) decrease in LAOS  $\omega$  results in greater crystal orientation. We anticipate that imposition of LAOS generates local chain orientation and activates point nuclei (as in steady shear). For polymer crystals, it is reasonable that “point” nuclei have a plate-like geometry and that oscillatory flow might couple to their orientation. This coupling might account for the observed gradient orientation of lamellar structures. Indeed, for oblate (plate-like) ellipsoids subjected to shear in a viscous liquid, minimum energy arguments by Jeffery<sup>11</sup> suggest that the particles would eventually align with their axis in the gradient direction. This was experimentally verified by Taylor.<sup>12</sup> In more recent experiments on dense colloidal dispersions of plate-like particles, oscillatory shear has been demonstrated to be highly effective in aligning the particles with their axes along the flow gradient direction.<sup>13</sup>

Flow gradient orientation has also been demonstrated for a variety of ordered lamellar systems, from block copolymers<sup>14</sup> to small molecule and lyotropic smectic liquid crystals.<sup>15</sup> In lamellar diblock copolymers, it is well established that LAOS aligns the layers along the flow gradient at low  $\omega$ , along the vorticity direction at intermediate  $\omega$  and, in the gradient direction at higher  $\omega$ . In the LAOS experiments reported here, increasing  $\omega$  retards crystallization kinetics and decreases  $f$ , suggesting that the effect of LAOS on crystal orientation does not arise from shear-induced deformation of chain conformations. Rather, once plate-like nuclei form, it is likely that LAOS couples hydrodynamically with these to reorient them with their chain axis along the flow gradient direction. This also suggests that crystal lamellae will not be oriented as their Brownian reorientation time scale<sup>10</sup> approaches  $\omega^{-1}$ .

We explore the nature of the point nuclei, by imposing LAOS at different temperatures. There is currently no direct experimental evidence for the existence of flow-activated point nuclei. In isothermal LAOS experiments on RCP at 132 °C, we can detect no change in the melt rheology on imposition of LAOS. Our rheological measurements, however, show that the onset of crystallization occurs several thousand seconds after cessation of LAOS. When  $t_c$  is compared with the relaxation time  $\sim O(0.1\text{ s})$  of the RCP melt at 132 °C (SI, Figure S2), it is clear that imposition of LAOS must have resulted in the formation of structures that persist well beyond melt chain relaxation time scales. In our experiments, the formation of LAOS-induced structures is manifested at much later times after the cessation of shear in the orientation of the RCP crystals and in the decreased  $t_c$ . Such effects have been reported previously in the literature<sup>6,16,17</sup> and have been termed “melt memory”. We believe that this melt memory refers to the presence of shear-induced structures that defy direct detection

using currently available experimental techniques. We explore the melt memory effect using homopolymer (iPP) by cooling a melt at 240 °C to different shear temperatures and then imposing LAOS (SI, Experimental Details). We choose iPP with approximately the same  $M_w$  as RCP for these experiments to facilitate comparison with the literature. After imposition of LAOS, iPP is held isothermal for different time intervals, and is then cooled to room temperature at 10 °C/min, for it to crystallize. We do not perform isothermal crystallization experiments since the crystallization rate of the iPP is very slow at temperatures  $>140\text{ °C}$ .

In iPP, as in RCP, we observe that imposition of LAOS results in crystal orientation in the flow gradient direction. For 8 cycles of LAOS ( $\omega = 1\text{ rad}\cdot\text{s}^{-1}$ ,  $\gamma = 250\%$ ), samples cooled to room temperature immediately after imposition of shear show crystal orientation in the gradient direction for shearing temperatures as high as 180 °C, namely, 15 °C above the iPP nominal melting point (Figure 3). This is in accord with

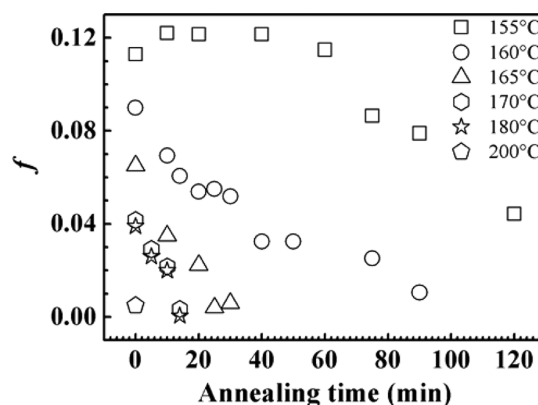


**Figure 3.** Decrease in the orientational order parameter as iPP is isothermally annealed after LAOS.

previous studies<sup>6</sup> that have demonstrated the formation of oriented shear-induced crystallization precursors for short-term shearing at temperatures above the nominal melting point of iPP. However, LAOS at 200 °C does not lead to the development of crystal orientation when cooled to room temperature. The orientational order parameter,  $f$ , for samples cooled immediately after LAOS, decreases with increase in the shearing temperature from  $\approx 0.12$  for 155 °C to  $\approx 0.04$  at 180 °C. When samples are annealed at the shearing temperature after cessation of LAOS,  $f$  decreases with an increase in annealing time. The decrease in  $f$  is more rapid at higher temperatures.

Decrease in  $f$  could result from “melting” of the LAOS-induced point nuclei or their orientational randomization by Brownian motion. For “point” nuclei that are plate-like, with a diameter,  $d$ , we estimate<sup>10</sup> the time for Brownian rotational diffusion to randomize their orientation as  $3k_B T/\eta d^3$ , where  $\eta$  is the matrix viscosity. At 160 °C, the decrease in  $f$  is characterized by a time of  $\approx 2860\text{ s}$ . For an iPP melt at 160 °C,  $\eta \approx 6 \times 10^3\text{ Pa}\cdot\text{s}$ . This gives an aphysical value for  $d \approx 4.7\text{ Å}$ , suggesting that Brownian orientational randomization does not govern the decrease in  $f$  on isothermal annealing. Further, we note that on cooling the sample immediately after cessation of LAOS at 160 °C, the iPP crystallization temperature increases to 126.8 °C,  $\approx 4\text{ °C}$  higher than if iPP was cooled directly from 160 °C, without shearing (123.2 °C, SI, Figure S12). This increase in crystallization temperature is not unexpected since we



anticipate that LAOS activated point nuclei would accelerate crystallization. If, however, the iPP is held at 160 °C for 90 min after imposition of LAOS, the iPP crystallizes at 123.8 °C. Thus, annealing at high temperatures after imposition of LAOS appears to melt the shear-activated point nuclei rather than randomize their orientation. Remarkably, the time scale that characterizes the decrease in  $f$  is similar for iPP and RCP (SI, Figure S13).

The time scale for decay of  $f$  shows an Arrhenius temperature dependence (activation energy  $\approx 226$  kJ/mol; SI, Figure S14). Our results accord with literature values (between 150 and 300 kJ/mol) for relaxation of crystal precursors.<sup>16,17</sup> Thus, the LAOS-generated structures appear to be similar to previously reported shear-induced crystallization precursors. While these precursors initiate the formation of flow-oriented shish structures in steady shear, LAOS appears to align the precursors with their chain axis (viz., plate axis) along the gradient direction.

These results provide insights into the nature of flow-activated point nuclei, and suggest how hitherto unreported crystal orientation can be obtained by imposition of LAOS. Qualitatively similar gradient orientation is observed for RCP, isotactic polypropylenes of different molecular weights and HDPE, suggesting that the phenomenon reported here is valid generally for semicrystalline polymers. (SI, Figures S15 and S16). Our results have implications for understanding the enhanced properties obtained from processing techniques such as SCORIM<sup>18</sup> (Shear Controlled Orientation Injection Molding), where application of an oscillatory stress on the crystallizing polymer melt during solidification in the mold results in enhanced crystallinity, crystal orientation, and in a simultaneous increase in the stiffness and toughness of molded objects.

## ■ ASSOCIATED CONTENT

### Supporting Information

Polymer characterization; crystallization kinetics; SAXS orientation. This material is available free of charge via the Internet at <http://pubs.acs.org>.

## ■ AUTHOR INFORMATION

### Corresponding Author

\*Tel.: +91-20-2590-2182. Fax: +91-20-2590-2618. E-mail: [g.kumaraswamy@ncl.res.in](mailto:g.kumaraswamy@ncl.res.in)

### Notes

The authors declare no competing financial interest.

## ■ ACKNOWLEDGMENTS

We are grateful to Reliance Industries Limited for the RCP and iPP samples and Dr. R. B. Basargekar for discussions. We are also grateful to Anuya Nisal and S. Karthika for their help with microstructural characterization.

## ■ REFERENCES

- (1) Middleman, S. *Fundamentals of Polymer Processing*; McGraw-Hill: New York, 1977.
- (2) Kumaraswamy, G. J. *Macromol. Sci., Polym. Rev.* **2005**, *45*, 375. Meerveld, van J.; Peters, G. W. M.; Hutter, M. *Rheol. Acta* **2004**, *44*, 119.
- (3) Keller, A.; Kolnaar, H. W. H. Flow-induced orientation and structure formation. In *Materials Science and Technology: A Comprehensive Treatment*; Meijer, H. E. H., Ed.; VCH: New York; Vol. 18, pp 191–268.

(4) Rastogi, S.; Yao, Y.; Ronca, S.; Bos, J.; van der Eem, J. *Macromolecules* **2011**, *44*, 5558.

(5) Shen, S.; Henry, A.; Tong, J.; Zheng, R.; Chen, G. *Nat. Nanotechnol.* **2010**, *5*, 251.

(6) Liedauer, S.; Eder, G.; Janeschitz-Kriegl, H.; Jerschow, P.; Geymayer, W.; Ingolic, E. *Int. Polym. Process.* **1993**, *8*, 236. Kumaraswamy, G.; Issaian, A. M.; Kornfield, J. A. *Macromolecules* **1999**, *32*, 7537. Somani, R. H.; Hsiao, B. S.; Nogales, A.; Srinivas, S.; Tsou, A. H.; Sics, I.; Balta-Calleja, F. J.; Ezquerro, T. A. *Macromolecules* **2000**, *33*, 9385. Pogodina, N. V.; Lavrenko, V. P.; Srinivas, S.; Winter, H. H. *Polymer* **2001**, *42*, 9031. Kumaraswamy, G.; Kornfield, J. A.; Yeh, F.; Hsiao, B. S. *Macromolecules* **2002**, *35*, 1762. Azzuri, F.; Alfonso, G. C. *Macromolecules* **2005**, *38*, 1723. Ogino, Y.; Fukushima, H.; Takahashi, N.; Matsuba, G.; Nishida, K.; Kanaya, T. *Macromolecules* **2006**, *39*, 7617. Kimata, S.; Sakurai, T.; Nozue, Y.; Kasahara, T.; Yamaguchi, N.; Karino, T.; Shibayama, M.; Kornfield, J. A. *Science* **2007**, *316*, 1014. Meng, K.; Dong, X.; Hong, S.; Wang, X.; Cheng, H.; Han, C. C. *J. Chem. Phys.* **2008**, *128*, 024906. Mykhaylyk, O. O.; Chambon, P.; Impradice, C.; Fairclough, J. P. A.; Terrill, N. J.; Ryan, A. J. *Macromolecules* **2010**, *43*, 2389. Shen, B.; Liang, Y.; Kornfield, J. A.; Han, C. C. *Macromolecules* **2013**, *46*, 1528.

(7) Wolkowicz, M. J. *Polym. Sci., Polym. Symp.* **1978**, *63*, 365.

(8) Doi, M.; Edwards, S. F. *The Theory of Polymer Dynamics*; Clarendon Press: Oxford, 1986.

(9) Hofl, A.; Kremer, F.; Spiess, H. W.; Wilhelm, M.; Kahle, S. *Polymer* **2006**, *47*, 7282.

(10) Larson, R. G. *The Structure and Rheology of Complex Fluids*; Oxford University Press: New York, 1999; pp 281.

(11) Jeffery, G. B. *Proc. R. Soc. London, Ser. A* **1922**, *102*, 161.

(12) Taylor, G. I. *Proc. R. Soc. London, Ser. A* **1923**, *103*, 58.

(13) Brown, A. B. D.; Rennie, A. R. *Phys. Rev. E* **2000**, *62*, 851.

(14) Koppi, K. A.; Tirrell, M.; Bates, F. S.; Almdal, K.; Colby, R. H. *J. Phys. II* **1992**, *2*, 1941. Chen, Z. R.; Kornfield, J. A.; Smith, S. D.; Grothaus, J. T.; Satkowski, M. M. *Science* **1997**, *277*, 1248.

(15) Larson, R. G.; Winey, K. I.; Patel, S. S.; Watanabe, H.; Bruinsma, R. *Rheol. Acta* **1993**, *32*, 245. Penfold, J.; Staples, E.; Lodhi, A. K.; Tucker, I.; Tiddy, G. J. T. *J. Phys. Chem. B* **1997**, *101*, 66. Zipfel, J.; Berghausen, J.; Lindner, P.; Richtering, W. *J. Phys. Chem. B* **1999**, *103*, 2841.

(16) Alfonso, G. C.; Scardigli, P. *Macromol. Symp.* **1997**, *118*, 323. Janeschitz-Kriegl, H. *Colloid Polym. Sci.* **1997**, *275*, 1121. Cavallo, D.; Azzurri, F.; Balzano, L.; Funari, S. S.; Alfonso, G. C. *Macromolecules* **2010**, *43*, 9394.

(17) Isayev, T.; Chan, W.; Shimojo, K.; Gmerek, M. J. *Appl. Polym. Sci.* **1995**, *55*, 807.

(18) Kalay, G.; Bevis, M. J. *J. Polym. Sci., Part B: Polym. Phys.* **1997**, *35*, 241.